Appl. Phys. B (2017) 123:45
DOI 10.1007/s00340-016-6618-2

Applied Physics B
Lasers and Optics

Realizing three-step photoionization of calcium by two lasers

Jie Zhang[1,2] · Yi Xie[2] · Peng-fei Liu[2] · Bao-quan Ou[2] · Wei Wu[1,2] · Ping-xing Chen[1,2]

Received: 26 December 2015 / Accepted: 8 December 2016 / Published online: 13 January 2017

Abstract In this paper, we report a new method to load $^{40}Ca^{+}$ into ion traps. We show that the three-step photoionization process, which is stimulated by laser light at 423, 732 and 830 nm, can be realized by two lasers at 423 and 732 nm. Compared to the original three-step method, the new scheme has a more simple experimental setup and similar loading efficiency can be achieved with proper laser parameters. The loading efficiency as a function of the 732 nm laser power and detuning is also experimentally investigated.

1 Introduction

Quantum computing with cold trapped ions was proven to be one of the most promising methods for realizing scalable quantum information processing (QIP) [1, 2]. As a popular ion for QIP experiments [3–6], $^{40}Ca^{+}$ has a hyperfine free structure and all of the lasers required can be obtained from commercial diode laser products. Additionally, trapped cold $^{40}Ca^{+}$ shows great potential in precision spectroscopy research [7–9].

The traditional method of creating ions in an ion trap is electron bombardment (EB). However, there are many disadvantages when using this method. First, EB has no isotopic selectivity and may ionize the residual gas in the trap volume. Second, the atomic flux for EB loading deposits on the dielectrics during the loading process could induce serious heating problems [10, 11]. Finally, the number of ions loaded cannot be controlled. This defect results in problems in experiments where specific numbers of ions are required [12–14].

To solve the problems caused by EB loading, photoionization has been developed to load ions [15–23]. For calcium photoionization, a resistively heated oven ejects the neutral calcium beam into the trap center, where atoms can be ionized by one, two or three lasers. Figure 1 shows several common laser-induced ionization schemes for calcium atoms. We can use a single laser beam to implement the calcium loading as long as the laser wavelength meets the requirements of multi-photon resonance [15–17], but it is not feasible in practice due to the high price and technical requirements. The two-photon photoionization schemes are more common. In these methods, the dipole transition $4s4s\ ^1S_0 \leftrightarrow 4s4p\ ^1P_1$ of neutral calcium is excited by laser light at 423 nm and followed by excitation to the autoionizing state with a laser light under 390 nm [18–21]. It is demonstrated that the efficiency of the photoionization is independent of the linewidth of the laser light used in the second step [20]. As a result, sufficient loading rates can also be reached with a laser at 423 nm and an LED with central wavelength below 390 nm [22, 23], as shown in Fig. 1(II). Although the LED is a favorable device for calcium loading in macroscopic ion traps, large beam divergence limits its application in microtraps, because there is normally only tens of microns between the trap center and the electrode surface [24, 25]. Furthermore, the potential drift caused by the light-induced charging [26] effect of ultraviolet (UV) lasers leads to frequent compensations for the micromotion.

✉ Ping-xing Chen
pxchen@nudt.edu.cn

[1] State Key Laboratory of High Performance Computing, National University of Defense Technology, Changsha 410073, Hunan, People's Republic of China

[2] Department of Physics, College of Science, National University of Defense Technology, Changsha 410073, Hunan, People's Republic of China

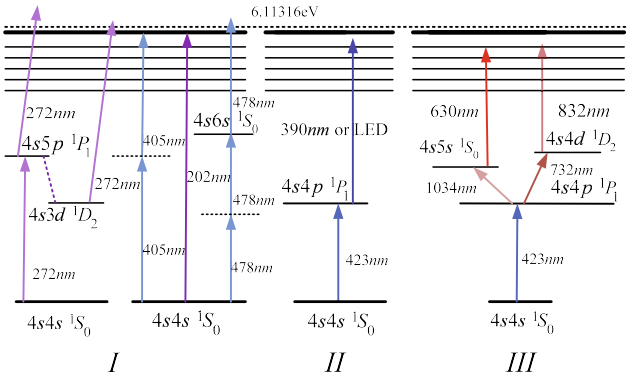

Fig. 1 Three possible kinds of laser-induced calcium ionization routes. The classification is based on the number of laser beams used in the experiment. (*I*) Calcium ionized via excitation of a single laser field at the wavelength of 202, 272, 405 or 478 nm; (*II*) The most common two-step schemes realized via the laser field of 423 nm and the laser (LED) field under 390 nm; (*III*) Three-step schemes implemented with the laser field of 423 nm and other two infrared laser fields at the wavelength of 732 nm (1034 nm) and 830 nm (630 nm)

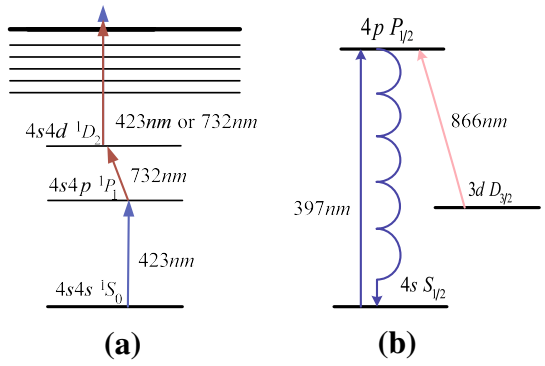

Fig. 2 **a** Relevant energy levels of our photoionization scheme. The photoionization is realized by excitation of the $4s4s\ ^1S_0 \leftrightarrow 4s4p\ ^1P_1$ dipole transition at 423 nm, followed by stimulation to $4s4d\ ^1D_2$ with a 732 nm laser beam, and finally, by the excitation of 423 or 732 nm photons. **b** Energy levels and laser wavelengths for the Doppler cooling of ^{40}Ca ion

To obtain experimentally feasible laser beams and eliminate the problem caused by UV lasers, three-step photoionization [27] schemes are proposed, as shown in Fig. 1(III). However, a three-step scheme requires three laser beams and a more complicated optical setup, which means the three-step photoionization schemes are still not an ideal method for loading calcium ions.

We propose a scheme that utilizes two lasers to realize three-step photoionization of calcium. This scheme not only has a more simple experimental setup but also can eliminate the problems caused by UV lasers compared to the two-step scheme. Experimental results show that the efficiency of the new scheme is acceptable for loading calcium ions. Moreover, the frequency and power dependences of the $4s4p\ ^1P_1 \leftrightarrow 4s4d\ ^1D_2$ transition are investigated in our experiments.

2 Ionization scheme and experimental setup

Our ionization scheme for calcium is shown in Fig. 2. First, the 423 nm laser field drives the dipole transition from the ground $4s4s\ ^1S_0$ state to the intermediate $4s4p\ ^1P_1$ state (Γ_P= 34.7 MHz). Then the cascade process is stimulated with a 732 nm laser, by which the atoms are excited from the $4s4p\ ^1P_1$ state to the $4s4d\ ^1D_2$ state(Γ_D = 2.29 MHz). Finally, the atoms are ionized by absorbing a 732 or 423 nm photon.

According to the atomic data for calcium in the database of NIST [27], the energy for removing one of the valence electrons out of atomic calcium is 6.11316 eV. The 423 nm photons provide 2.9326 eV to excite the atoms to $4s4p\ ^1P_1$ state, then the 732 nm photons with 1.6918 eV stimulate the atoms to $4s4d\ ^1D_2$. After absorbing the 423 and 732 nm photons, the atoms can be ionized by photons with energies more than 1.48876 eV (the corresponding laser wavelength is 832 nm), and hence in our scheme, the 830 nm laser can be replaced by the 732 nm laser or 423 nm laser; in other words, the ionization can be realized without 830 nm laser.

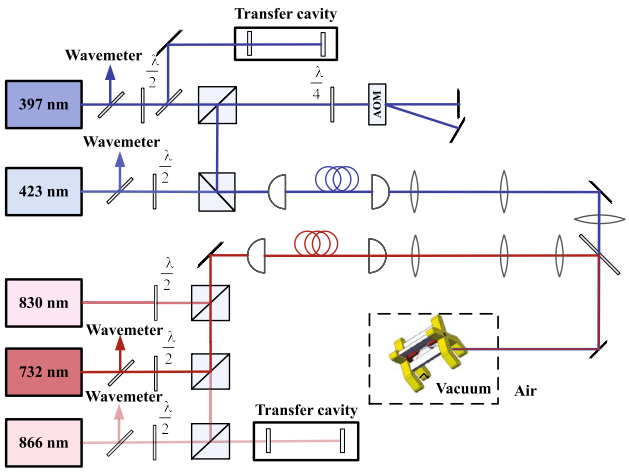

Fig. 3 The setup of the calcium photoionization experiment. All of the lasers are diode lasers and wavelengths are monitored by using a wavemeter with an opto-mechanical switch. The frequencies of the Doppler cooling lasers at 397 and 866 nm are stabilized by transfer cavities. All of these laser beams are overlapped by a dichroic laser beam combiner before finally transmitting to the ion trap. The lens are used to adjust the waists of the laser beams

The ion trap used in this work is in a blade-shaped configuration with r_{trap}=1.13 mm and l_{trap}=5 mm [28]. The ion trap is mounted in a vacuum chamber, which is pumped by an ion pump and a titanium sublimation pump, with a

measured vacuum pressure below 3×10^{-10} mbar. The oven is positioned under the ion trap at 90° with respect to the trap axis. The distance between the nozzle of the oven and the trap center is about 2 cm. A radio frequency signal is coupled to the trap through a quarter-wave helical resonator. For a single ion, the secular frequency is $2\pi \times 1.2$ MHz in the transverse and $2\pi \times 0.45$ MHz in the axial direction with endcap voltage at 200 V.

Figure 3 shows the simplified setup of the calcium photoionization experiment. All of the lasers used in our experiments are external-cavity grating stabilized diode lasers, except the free running 830 nm diode laser, which has no grating. The long term drift of the Doppler cooling lasers at 397 and 866 nm are suppressed by locking them to the transfer cavities, which are referenced to an ultrastable 729 nm laser source. Both the 423 and 732 nm lasers have good frequency performance with frequency changes within 12 MHz per 10 min. Fluorescence detection is provided by a 397 nm laser beam red detuned by 200 MHz from the resonant frequency of the dipole transition $4s4s\ ^1S_2 \leftrightarrow 4s4s\ ^1P_1$. Due to the large branching ratio, The 866 nm laser set at resonant is used to repump the ion out of the metastable $D_{3/2}$ state, as shown in Fig. 2b. The saturation parameter of the 397 nm (866 nm) is about 15 (235) to provide sufficient cooling for the newly loaded ions. To minimize the modifications on the whole experimental setup, the 397 and 423 nm laser beams are coupled to one fiber, while the 732, 830 and 854 nm beams are coupled to another fiber. All of these laser beams are overlapped by a dichroic laser beam combiner and focused at trap center with waist sizes of about 40 μm for the 397, 423 nm laser beams and 45 μm for the 732, 830, 854 nm laser beams. The powers of the 423 and 830 nm lasers are held constant at 1 and 2 mW, respectively. The power of the 732 nm laser can be adjusted from 0 to 1.5 mW using an attenuator.

3 Loading of ions

To determine the optimal current for the oven, we slowly increase the current through the oven and use an EMCCD with an optical bandpass filter at 423 nm to detect the photons emitted by the $4s4s\ ^1S_0 \leftrightarrow 4s4p\ ^1P_1$ dipole transition. The proper working current at 2.85 A is found when weak fluorescence is detected. Since the 423 nm laser has a power of 1 mW and a waist of 40 μm, its optical intensity in units of saturation intensity is 54 and the corresponding saturated absorption linewidth is $\Gamma' = \Gamma_P\sqrt{1 + I/I_0} = 262$ MHz, which is in the good range for isotopically loading ^{40}Ca ions [20]. The 732 nm laser is initially operated at 1 mW in our loading. Figure 4 shows the single trapped ion created by using the two lasers driving three-step photoionization scheme.

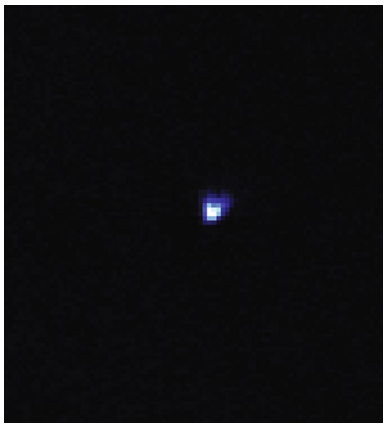

Fig. 4 Single trapped ^{40}Ca ion produced by the 423 and 732 nm lasers

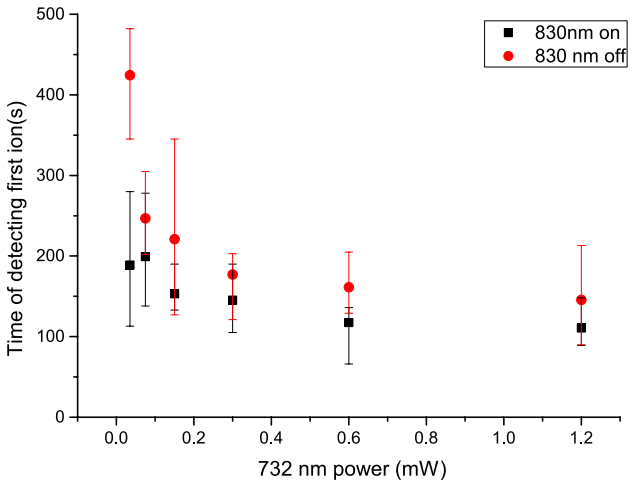

Fig. 5 The loading efficiency (average time of loading single ion) plotted as a function of the 732 nm laser power. *Each point* means the average time for six experiments and the *bars* indicate the measured maximum and minimum time of detecting the first ion. The *red dots* indicate the result without the 830 nm laser, while the *black dots* represent the time with the 830 nm laser

4 Laser stimulation parameters on loading efficiency

Since several experiments have studied the properties of the $4s4s\ ^1S_0 \leftrightarrow 4s4p\ ^1P_1$ dipole transition in the first step [19, 20], we focus on the properties of the $4s4p\ ^1P_1 \leftrightarrow 4s4d\ ^1D_2$ transition in the second step and keep the stimulation parameters of the first step unchanged. In this section, we will study the loading efficiency as a function of the power and detuning of the 732 nm laser.

In the first experiment, the loading efficiency as a function of the 732 nm laser power is studied. The loading efficiency is evaluated based on the time interval from the heating

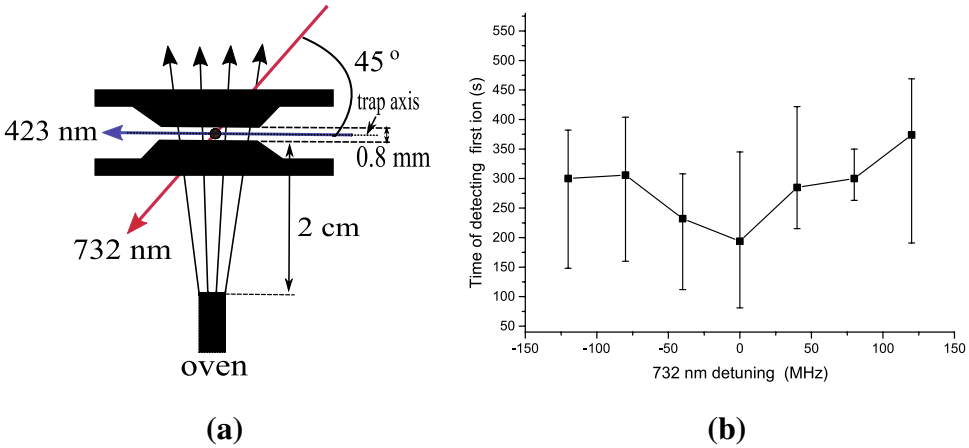

Fig. 6 **a** Setup of the photoionization laser beams and the region near trap center in the upgraded system. The 732 nm laser beam makes a 45° angle with the atomic beam axis, and the 423 nm laser beam is perpendicular to the atomic beam axis; **b** The loading efficiency (average time of loading a single ion) as a function of the frequency of the 732 nm laser. The *bars* indicate the maximum and minimum time of detecting the first ion. The 423 nm laser intensity is about 200 mW/mm^2. The 732 nm laser intensity is 6.3 mW/mm^2 , which is about a factor of 140 larger than its saturation intensity 0.045 mW/mm^2

of the atomic calcium oven to loading of the first ion. The results are plotted in Fig. 5. Each test point is the average time of six independent experiments, and the bars in the figure indicate the maximum and minimum time of detecting the first ion. Because the 732 nm laser power intensity varies from 10.8 to 0.35 mW/mm^2, which is far more than its saturation intensity of 0.045 mW/mm^2, the improvement in the loading efficiency with increasing laser power seems to correspond to the enhancement in the third step. This is verified by introducing the 830 nm laser in the experiments. As shown in Fig. 5, there is a significant efficiency improvement for each point with the 830 nm laser beam, especially when the 732 nm laser power is low. It is also important to note that the enhancement is not obvious when the 732 nm laser power is greater than 1 mW. Therefore, high loading rates can be reached with a high 732 nm laser power.

Apart from the laser power of 732 nm, the loading efficiency may still be affected by its frequency. In the following experiment, the loading efficiency as a function of the frequency of the 732 nm laser is investigated. The laser beam setup is different from that of the first experiment due to the upgrade of the experimental system. As shown in Fig. 6a, the 423 nm laser beam and the trap axis are in parallel, while the 732 nm beam is at a 45° angle with respect to the trap axis. Experimentally, the 423 nm laser intensity is approximately 200 mW/mm^2 and the 732 nm laser intensity is 6.3 mW/mm^2, which is approximately a factor of 140 larger than its saturation intensity 0.045 mW/mm^2.

Figure 6b shows the loading efficiency as a function of the 732 nm detuning. Each point indicates the average time of three independent measurements, and the bar represents the maximum and minimum time of detecting the first ion. As shown in the graph there is not a strong dependence of the absorption linewidth on the 732 nm laser detuning. In addition, the linewidth is broadened tremendously due to the intensity broadening and Doppler broadening effects since the relatively hot atomic beam is not emitted perpendicular to the heavily saturated 732 nm laser beam as shown in Fig. 6a. Moreover, the line shape is complicated by the velocity-selective trapping of the ionized atoms in the ion traps because ions with kinetic energy larger than the depth of the trap well cannot be trapped.

5 Conclusion

We have demonstrated a new effective photoionization method for loading ^{40}Ca ions. The experimental results reveal the laser power and frequency dependencies of loading efficiency in the $4s4p\,^1P_1 \leftrightarrow 4s4d\,^1D_2$ dipole transition. An acceptable efficiency can be achieved with the combination of 423 and 732 nm lasers by properly choosing the parameters. Although not experimentally demonstrated, the same scheme could be used to load other isotopes of calcium with different laser frequencies. This method is of great value for ion trap researchers who use calcium ion as research candidates. In addition to avoiding the problems of the electron bombardment method and reducing the cost, this new loading scheme can help eliminate the problems of using UV light [6, 29].

Acknowledgements This work is supported by The National Key Research and Development Program of China (2016YFA0301903), The National Natural Science Foundation of China (NSFC)

(11174370, 61205108) and Open Project Program of the State Key Laboratory of High Performance Computing (201301-01).

References

1. J.I. Crac, P. Zoller, Phy. Rev. Lett. **74**, 4091 (1995)
2. S. Debnath, N.M. Linke, C. Figgatt, K.A. Landsman, K. Wright, C. Monroe, Nature **536**, 63 (2016)
3. C.F. Roos, M. Riebe, H. Häffner, W. Hänsel, J. Benhelm, G.P.T. Lancaster, C. Becher, F. Schmidt-Kaler, R. Blatt, Science **304**, 1478 (2004)
4. T. Monz, P. Schindler, J.T. Barreiro, M. Chwalla, D. Nigg, W.A. Coish, M. Harlander, W. Hänsel, M. Hennrich, R. Blatt, Phys. Rev. Lett. **106**, 130506 (2011)
5. A.S. Schulz, U. Poschinger, F. Ziesel, F. Schmidt-Kaler, New J. Phys. **10**, 045007 (2008)
6. A.H. Myerson, D.J. Szwer, S.C. Webster, D.T.C. Allcock, M.J. Curtis, G. Imreh, J.A. Sherman, D.N. Stacey, A.M. Steane, D.M. Lucas, Phys. Rev. Lett. **100**, 200502 (2008)
7. P.L. Liu, Y. Huang, W. Bian, H. Shao, H. Guan, Y.-B. Tang, C.-B. Li, J. Mitroy, K.-L. Gao, Phys. Rev. Lett. **114**, 223001 (2015)
8. Y. Wan, F. Gebert, J.B. Wübbena, N. Scharnhorst, S. Amairi, I.D. Leroux, B. Hemmerling, N. Lörch, K. Hammerer, P.O. Schmidt, Nat. Commun. **5**, 3096 (2014)
9. Y. Huang, J. Cao, P. Liu, K. Liang, B. Ou, H. Guan, X. Huang, T. Li, K. Gao, Phys. Rev. A **85**, 030503 (2012)
10. D.J. Wineland, C. Monroe, W.M. Itano, D. Leibfried, B.E. King, D.M. Meekhof, J. Res. Natl. Inst. Stand. Technol. **103**, 259 (1998)
11. L. Deslauriers, P.C. Haljan, P.J. Lee, K.A. Brickman, B.B. Blinov, M.J. Madsen, C. Monroe, Phys. Rev. A **70**, 043408 (2004)
12. B.E. King, C.S. Wood, C.J. Myatt, Q.A. Turchette, D. Leibfried, W.M. Itano, C. Monroe, D.J. Wineland, Phys. Rev. Lett. **81**, 1525 (1998)
13. H.C. Nägerl, W. Bechter, J. Eschner, F. Schmidt-Kaler, R. Blatt, Appl. Phys. B **66**, 603 (1998)
14. S. An, J.-N. Zhang, M. Um, D. Lv, Y. Lu, J. Zhang, Z.-Q. Yin, H.T. Quan, K. Kim, Nat. Phys. **11**, 193 (2015)
15. N. Kjærgaard, L. Hornekær, A.M. Thommesen, Z. Videsen, M. Drewsen, Appl. Phys. B **71**, 207 (2000)
16. R.S. Dygdala, K. Karasek, F. Giammanco, J. Kobus, A. Pabjanek-Zawadzka, A. Raczyński, J. Zaremba, M. Zieliński, J. Phys. B At. Mol. Opt. Phys. **31**, 2259 (1998)
17. R.J. Hendricks, D.M. Grant, P.F. Herskind, A. Dantan, M. Drewsen, Appl. Phys. B **88**, 507 (2007)
18. C. Schuck, F. Rohde, M. Almendros, M. Hennrich, J. Eschner, Appl. Phys. B **100**, 765 (2010)
19. S. Gulde, D. Rotter, P. Barton, F. Schmidt-Kaler, R. Blatt, W. Hogervorst, Appl. Phys. B **73**, 861 (2001)
20. D.M. Lucas, A. Ramos, J.P. Home, M.J. McDonnel, S. Nakayama, J.-P. Stacey, S.C. Webster, D.N. Stacey, A.M. Steane, Phys. Rev. A **69**, 012711 (2004)
21. T.R. Gentile, B.J. Hughey, D. Kleppner, T.W. Ducas, Phys. Rev. A **40**, 5103 (1989)
22. U. Tanaka, H. Matsunishi, I. Morita, S. Urabe, Appl. Phys. B **81**, 795 (2005)
23. U. Tanaka, I. Morita, S. Urabe, Appl. Phys. B **89**, 195 (2007)
24. K. Wright, J.M. Amini, D.L. Faircloth, C. Volin, S.C. Doret, H. Hayden, C.-S. Pai, D.W. Landgren, D. Denison, T. Killian, R.E. Slusher, A.W. Harter, New J. Phys. **15**, 033004 (2013)
25. D.A. Craik, N.M. Linke, T.P. Harty, C.J. Ballance, D.M. Lucas, A.M. Steane, D.T.C. Allcock, Appl. Phys. B **114**, 3 (2013)
26. M. Harlander, M. Brownnutt, W. Hänsel, R. Blatt, New J. Phys. **12**, 093035 (2010)
27. C. Corliss, J. Sugar, J. Phys. Chem. Ref. Data 14(Suppl 2) (1985)
28. S.T. Gulde, PhD thesis, Universität Innsbruck (2003)
29. D.T.C. Allcock, T.P. Harty, H.A. Janacek, N.M. Linke, C.J. Ballance, A.M. Steane, D.M. Lucas, R.L. Jarecki Jr., S.D. Habermehl, M.G. Blain, D. Stick, D.L. Moehring, Appl. Phys. B **107**, 913 (2012)